JOURNAL OF MATERIALS SCIENCE 26 (1991) 3366–3373

Crystallization of some spodumene–lithium zinc orthosilicate glasses

A. A. OMAR, A. W. A. EL-SHENNAWI, A. R. EL-GHANNAM
National Research Centre, Dokki, Cairo, Egypt

By using thermal analysis, X-ray diffraction, polarizing and electron microscopy the effect of compositional variation, thermal treatment and nucleation catalysts TiO_2 and ZrO_2 on the nature, type and stability fields of the crystallizing phases, as well as the resulting microstructures, is described for some stoichiometric glass compositions within the system $LiAlSi_2O_6$–Li_2ZnSiO_4. Intense uniform volume crystallization was achieved. Transparent glass-ceramics with ultrafine microstructures could also be obtained at temperatures near 700 °C. Crystallization begins with the formation of a proto β- and/or $\beta_{II'}$-Li_2ZnSiO_4 followed by, or concomitant with, β-eucryptite ss. The proto β-phase was formed over a narrow temperature range and rapidly transformed into its $\beta_{II'}$-modification which, although showing a wider stability range, ultimately transformed into the stable γ_0-modification. The metastable β-eucryptite ss starts its transformation into β-spodumene around 800 °C. By prolonged heating at temperatures as high as 1000–1040 °C, β-spodumene and γ_0-Li_2ZnSiO_4 were the main stable end products. TiO_2 and ZrO_2 have contrasting effects on the stability of the LiZn orthosilicates and β-eucryptite ss → β-spodumene transformations. The former exhibits a catalytic effect and the latter showed a retarding effect on these processes.

1. Introduction

Glass-ceramics are polycrystalline materials resulting from the controlled crystallization of specially formulated glasses [1, 2]. The properties of a glass-ceramic body are determined both by the properties of the crystalline phase(s) and microstructures which appear during heat treatment. The role of nucleating catalysts [1–5] in initiating crystallization from a multitude of centres is the most determining factor in glass-ceramic production. As the number of possible phases increases, the probability of production of fine-grained microstructures increases as well.

β-eucryptite solid solution(s) (ss) and β-spodumene ss are among the most promising low-expansion glass-ceramic-forming phases and therefore have attracted considerable attention [1–5]. The lithium zinc orthosilicates also have attractive properties [6–9].

No work relating spodumene and lithium zinc orthosilicates to each other is yet known. The purpose of the present work was to describe how glasses of selected compositions in the system $LiAlSi_2O_6$–Li_2ZnSiO_4 behave at different heat-treatment temperatures, as well as the effect of TiO_2 and ZrO_2 on their crystallization and microstructures.

2. Experimental procedure

2.1. Compositions and glass preparation

Some glass compositions within the system spodumene–lithium zinc orthosilicate were selected for the present investigation (Table I). Glasses with more than 50 mol % Li_2ZnSiO_4 devitrified into white opaline bodies on quenching in air and were thus excluded.

Acid-washed pulverized quartz and analytical reagents Li_2CO_3, ZnO, Al_2O_3, TiO_2 and ZrO_2 were used as batch materials. The weighed proportions were thoroughly mixed and melted in platinum crucibles in a globar furnace at 1400 °C for 3 h. Homogeneity of the melt was achieved by swirling the

TABLE I Composition of the base glasses

Glass no.	Nominal phase composition (mol %)		Constituent oxides (wt %)				Yield
	Li_2ZnSiO_4 ($\beta_{II'}$)	$LiAlSi_2O_6$	Li_2O	ZnO	Al_2O_3	SiO_2	
G2	20	80	9.79	8.89	22.27	59.05	Clear glass
G4	40	60	11.61	18.06	16.98	53.35	Clear glass
G5	50	50	12.54	22.77	14.26	50.43	Brilliant clear glass
G6	60	40	13.49	27.55	11.50	47.46	Devitrified

melt-containing crucible several times at about 20 min intervals and was ensured in the resultant glass by microscopic examination. The melt was cast into 10 cm x 1 cm x 1 cm rods and as buttons which were then properly annealed in a muffle furnace.

2.2. Thermal treatments

The progress of crystallization was investigated in samples subjected to (i) single- and (ii) double-stage heat treatments. In the first schedule, glass buttons were reheated in a muffle furnace to the defined temperature in the 600–1050 °C temperature range at 30 or 60 °C intervals for 1, 3 and sometimes 20 h. In the second schedule, the specimens were first heated, according to the DTA results, at the endothermic peak temperature and this was followed by another treatment at the exothermic peak temperature. Further details of the actual heat-treatment cycles concerned are given with each of the glasses studied.

2.3. Differential thermal analysis (DTA)

80 mg powdered glass sample (− 0.60 and + 0.25 mm), a heating rate of 20 °C min^{-1} and sensitivity setting of 20 μV in^{-1} were adopted through a Schimadzu DT-30 apparatus.

2.4. X-ray diffraction analysis (XRD)

Powder X-ray diffraction patterns were obtained using a Phillips X-ray diffractometer type PW 1050, adopting Ni-filtered Cu radiation, operated at 36 kV and 16 mA. All the instrument settings were maintained for all the analyses and an external standard, namely a silicon disc, was always used to test this maintenance.

2.5. Polarizing microscopy

The mineralogical constitution and microstructures of heat-treated samples were examined whenever possible in thin sections using a polarizing Carl–Zeiss research microscope.

2.6. Transmission electron microscopy

Representative electron micrographs were obtained using EM/O Zeiss transmission electron microscope adopting the preshadowed carbon replica technique.

3. Results

3.1. Crystallization of base glasses

The DTA curves (Fig. 1) showed an endothermic effect in the 500–600 °C temperature range which may indicate the molecular rearrangement phenomenon preceding glass crystallization, i.e. precrystallization stage [10]. As the Li_2ZnSiO_4 component in the glass composition is increased over 40%, the crystallization behaviour was markedly modified. The major exotherm, appearing in the 650–700 °C range in glasses G2 and G4 and characterizing the crystallization of lithium zinc orthosilicate and β-eucryptite ss, was modified into three distinct but less pronounced effects in the DTA curve of G5. This curve (Fig. 1c) shows a relatively major exotherm at 611 °C, a less pronounced one at 714 °C and an exothermic shoulder-like effect at 727 °C. Also, the minor high-temperature exothermic peak common to all the thermograms was displaced to a lower temperature (to 830 °C). The thermal effects, endothermic and exothermic, and the corresponding structural changes are summarized in Table II.

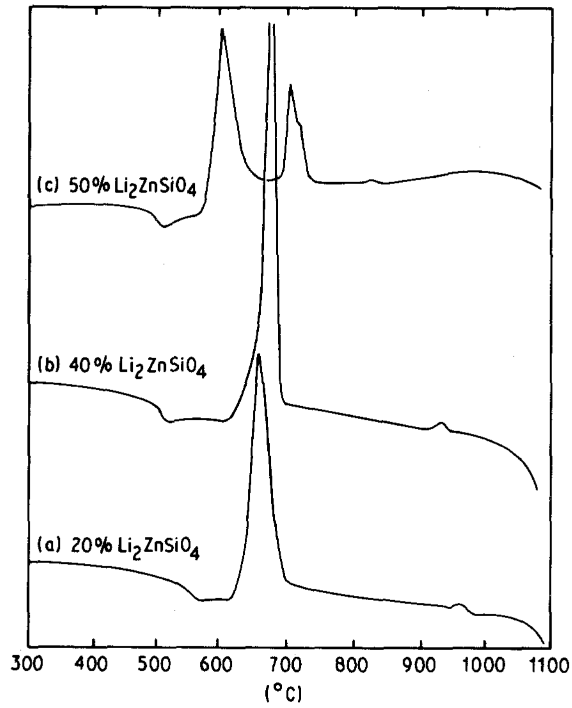

Figure 1 DTA curves of glasses of Li_2ZnSiO_4 + spodumene compositions.

Table III gives a short summary of the phases and microstructures developed in the heat-treated glasses as identified by X-ray powder diffraction and petrographic techniques.

Crystallization of both G2 and G4 glasses (with 20% and 40 mol % Li_2ZnSiO_4, respectively) resulted into the same assemblage of phases differing only, however, in their relative quantities and the resulting microstructures. More uniform fine-grained textures were displayed by the latter glass (G4) throughout the whole volume over a wide temperature range up to 1000 °C (Figs 2 and 3).

Glass samples of G4 were partially crystallized after 1 h heat treatment at 600 °C into considerable β-eucryptite ss and minor $\beta_{II'}$-Li_2ZnSiO_4. Further development of these phases took place at 650 °C. Double-stage heat treatment at the endothermic peak temperature (530 °C) for 1, 12, or 22 h followed by 1 h at the first exothermic peak (685 °C) resulted into the formation of the same crystalline phases as in the single-stage heat treatment, however, with finer microstructures. Upon heating at 800 °C for 3 h, the sample exhibited very fine bulk crystallization of tiny crystals of $\beta_{II'}$-Li_2ZnSiO_4 and β-eucryptite ss together with small amounts of β-spodumene. At 900 °C for 3 h, the

TABLE II Short summary of thermal effects in selected $LiAlSi_2O_6$–Li_2ZnSiO_4 glasses

Glass no.	Peak temp. (°C)	Thermal effect	Structural changes
G2	572	Shallow endothermic dip	Precrystallization structural rearrangements
	663	Strong exotherm	Cocrystallization of β-euc and $\beta_{II'}$
	963	Weak exotherm	Transformation $\beta_{II'} \rightarrow \gamma_0$
G4	534	Shallow endothermic dip	Precrystallization structural rearrangements
	686	Sharp strong exotherm	Cocrystallization of β-euc and $\beta_{II'}$
	940	Weak exotherm	$\beta_{II'} \rightarrow \gamma_0$ transformation
G%	521	Narrower shallow endothermic dip	Precrystallization structural rearrangements
	611	Strong exotherm	Formation of proto β-phase
	714	Moderate exotherm with shoulder	Formation of β-euc
	830	Minor exotherm	$\beta_{II'} \rightarrow \gamma_0$ transformation
G4 + 7% TiO_2	554	Deep endothermic valley	Precrystallization structural rearrangements
	606	Weak exothermic hump	Formation of proto β-phase
	630	High exotherm	Formation of β-euc
	678	Slight exothermic hump	Transformation of proto $\beta \rightarrow \beta_{II'}$
	721	Strong sharp exotherm	Formation of β-spod
	910	Slight exothermic break	Transformation of $\beta_{II'} \rightarrow \gamma_0$
	1026	Minor exotherm	Formation of rutile and Li_2TiSiO_5
G4 + 3% ZrO_2	552	Slight endothermic dip	Precrystallization structural rearrangements
	742	Strong exotherm	Formation of proto-β and β-euc
	794	Small exothermic hump	Transformation of proto-$\beta \rightarrow \beta_{II'}$
	829	Moderate sharp exotherm	Transformation of $\beta_{II'} \rightarrow \gamma_0$
	978	Minor exothermic effect	Transformation of β-euc → β-spod

β-eucryptite ss completely disappeared and was wholly converted to β-spodumene. At or slightly below this latter temperature the $\beta_{II'}$-Li_2ZnSiO_4 also began to transform to the γ_0-Li_2ZnSiO_4 phase. The X-ray analysis of this sample revealed β-spodumene, γ_0-Li_2ZnSiO_4 and traces of $\beta_{II'}$-Li_2ZnSiO_4. As the crystallization parameters (time and temperature) were increased the formation of γ_0-Li_2ZnSiO_4 was enhanced. On prolonged heating (20 h) at 1000 °C, the diffraction pattern became more distinct and revealed the stable β-spodumene and γ_0-Li_2ZnSiO_4 assemblage in amounts approaching their normal values (Table III).

Glasses with 50 mol % Li_2ZnSiO_4 (G5) crystallized in the bulk into uniform ultra-fine-grained microstructures, from which transparent glass-ceramic material could be obtained. The main primary crystalline phase developed in these transparent glass-ceramics was of the proto-β-lithium zinc orthosilicate type. Diffuse proto-β-Li_2ZnSiO_4 X-ray diffraction pattern was obtained for glass G5 yielding transparent glass-ceramics after heat treatment at 600 °C for 1 h. West and Glasser [6] attributed similar diffusibility to the minuteness of the proto-β crystallites. When this glass was subjected to higher temperature treatments (greater than 700 °C) it lost its transparency and was transformed into opaque very fine-grained crystalline material, with crystal size up to 1 μm. At or slightly above 650 °C, $\beta_{II'}$-LiZn orthosilicate and β-eucryptite ss were also developed in this sample and started their transformation to the corresponding stable modifications, β-spodumene and γ_0-Li_2ZnSiO_4, at about 750 and 850 °C, respectively. At 750 °C no proto-β-Li_2ZnSiO_4 phase was detected. However, the $\beta_{II'}$-phase, in this glass composition, persisted after treatments at temperatures as high as 1040 °C for 1 h, where the main diffraction lines of this phase were still present. Prolonged heating (20 h) at such elevated temperature (1040 °C) greatly intensifies the transformation of $\beta_{II'}$- into γ_0-Li_2ZnSiO_4.

3.2. Crystallization of titania nucleated glasses

Incorporation of TiO_2 in the glass noticeably modified its crystallization kinetics (Fig. 4). The DTA patterns were progressively complicated as the percentage of titania in the glass was increased. Introduction of 7% TiO_2 in the glass resulted in a decrease in the temperature of onset of crystallization by about 50 °C, (Table II).

Heat treatments of glass G4 nucleated by 7% TiO_2 at the 540 °C endothermic dip for 1 or 5 h did not show any signs of crystallization; however, glass-in-glass phase separation was observed after the 1 h treatment and was intensified after the 5 h treatments (Fig. 5).

Samples of this glass treated at 580, 600 or 620 °C for 1 h, or preheated at 540 °C for 1 h followed by 1/2 h at the already mentioned temperatures, were also transparent after heat treatment. However, X-ray diffraction analysis showed them to be partially crystalline and composed of proto-β-Li_2ZnSiO_4 (Fig. 6a). Heat treatment of this glass at 650 or 700 °C for 1 h also yields transparent glass-ceramic composed of ultra-fine crystallites (less than 100 nm) uniformly distributed in a glassy matrix (Fig. 7). The X-ray analysis (Fig. 6b) revealed some $\beta_{II'}$-Li_2ZnSiO_4 in addition to the β-eucryptite ss and proto-β-phase. Above 700 °C, both proto-β phase and β-eucryptite ss

TABLE III Crystalline phases and microstructures developed in the heat-treated Li_2ZnSiO_4–$LiAlSi_2O_6$ glasses

Glass composition	Heat-treatment parameters	Short description[a]
G2	650 °C, 3 h	Spherulites of β-euc and a surface rim of $\beta_{II'}$
	570 °C, 1 h + 660 °C, 1 h	Non-uniform microstructure of β-euc and $\beta_{II'}$ crystallites
	800 °C, 1 h	Similar to the above, but with some β-spod
	900 °C, 1 h	β-euc, β-spod, γ_0 and $\beta_{II'}$ intergrowths
	900 °C, 3 h	Subradiated intergrowths of β-spod, γ_0 and $\beta_{II'}$
G4	600 °C, 3 h	Coarse spheroides of β-euc with $\beta_{II'}$ crystallites at the prepheries
	650 °C, 3 h	Similar to the above
	530 °C, 22 h + 685 °C, 1 h	Cryptocrystalline material of β-euc and $\beta_{II'}$
	800 °C, 3 h	Bulk crystallization of tiny lithium zinc orthosilicate and β-euc with some skeletals of β-spod
	900 °C, 1 h	Fine bulk crystallization of β-spod, γ_0 and $\beta_{II'}$
	1000 °C, 20 h	Mainly β-spod and γ_0
G5	600 °C, 1 h	Microscopically isotropic, but XRD revealed proto-β
	650 °C, 3 h	Transparent glass-ceramic material, XRD revealed β-euc, proto-β and $\beta_{II'}$
	750 °C, 1 h	Translucent crystalline material of β-euc, $\beta_{II'}$ and β-spod
	850 °C, 1 h	Ultrafine crystalline mass of β-spod, γ_0 and $\beta_{II'}$ phases.
	1040 °C, 1 h	Very fine-grained crystalline mass of β-spod, γ_0 and $\beta_{II'}$
	1040 °C, 20 h	Similar, but only of β-spod and γ_0
G4 + 5% TiO_2	700 °C, 1 h	Hemicrystalline mass of minute β-euc and lithium zinc orthosilicate
	550 °C, 3 h + 700 °C, 1 h	Similar to the above
G4 + 7% TiO_2	540 °C, 1 h + 600 °C, $\frac{1}{2}$ h	Microscopically isotropic but XRD revealed proto-β
	600 °C, 1 h	Similar to the above
	540 °C, 1 h + 620 °C, 1 h	β-euc was developed beside the proto-β-phase
	700 °C, 1 h	Homogeneous ultrafine microstructure
	800 °C, 1 h	Nearly holocrystalline mass of β-spod and $\beta_{II'}$
	1000 °C, 3 h	β-spod, γ_0, rutile and lithium titanium silicate
G4 + 0.5% ZrO_2	535 °C, 1 h + 700 °C, 1 h	Uniform fine-grained microstructure of β-euc and $\beta_{II'}$
	535 °C, 5 h + 700 °C, 1 h	Similar to the above
G4 + 1.5% ZrO_2	545 °C, 1 h + 710 °C, 1 h	Cryptocrystalline mass of β-euc and $\beta_{II'}$
	545 °C, 1 h + 760 °C, 1 h	Fine β-euc crystals in a cryptocrystalline groundmass of $\beta_{II'}$ and γ_0
	545 °C, 1 h + 780 °C, 1 h	Similar to the above
	545 °C, 1 h + 950 °C, 1 h	Fine bulk crystallization of β-spod and γ_0
G4 + 3% ZrO_2	600 °C, 1 h	Crystalline film of proto-β
	550 °C, 1 h + 740 °C, 1 h	Bulk crystallization of β-euc, γ_0 and $\beta_{II'}$
	830 °C, 1 h	Similar to the above
	900 °C, 1 h	The above intergrowths are slightly developed but still ultrafine
	550 °C, 1 h + 980 °C, 1 h	Bulk crystallization of β-spod, γ_0 and traces of β-euc

[a] Crystalline phases were mainly identified by XRD. β-euc = β-eucryptite ss; β-spod = β-spodumene; $\beta_{II'} = \beta_{II'}$-$Li_2ZnSiO_4$; $\gamma_0 = \gamma_0$-Li_2ZnSiO_4; proto-β = proto-β-lithium zinc orthosilicate.

began to transform into $\beta_{II'}$-Li_2ZnSiO_4 and β-spodumene, respectively. The sample became translucent and the opacity steadily increased over a very limited temperature range whereby the 750 °C heat-treated samples were mostly opaque. Samples treated at 800 °C were nearly holocrystalline consisting of fair-sized intergrowths of β-spodumene and $\beta_{II'}$-Li_2ZnSiO_4 (Fig. 6c). The latter phase begins to transform into a γ_0-Li_2ZnSiO_4 phase above 800 °C. At relatively higher temperatures (either at 900 or 1000 °C for 1 h) β-spodumene and γ_0-Li_2ZnSiO_4 were the main crystalline phases (Fig. 6d) and only after 3 h treatment at 1000 °C the lines of rutile became more distinct in addition to the probable formation of a small amount of a Li_2TiSiO_5 phases (Fig. 6e).

Therefore, it follows that TiO_2 broadens the crystallization field of the proto-β-phase by enhancing its formation and/or retarding the formation of

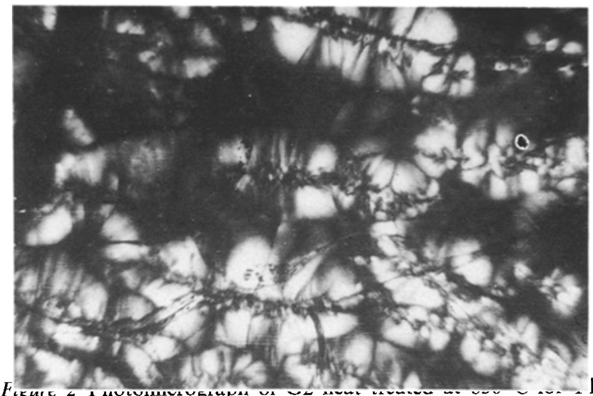

Figure 2 Photomicrograph of G2 heat treated at 650 °C for 1 h. Fair-sized β-eucryptite ss spherulites enclosing in between fine $\beta_{II'}$-Li_2ZnSiO_4 growths (crossed polars, × 60).

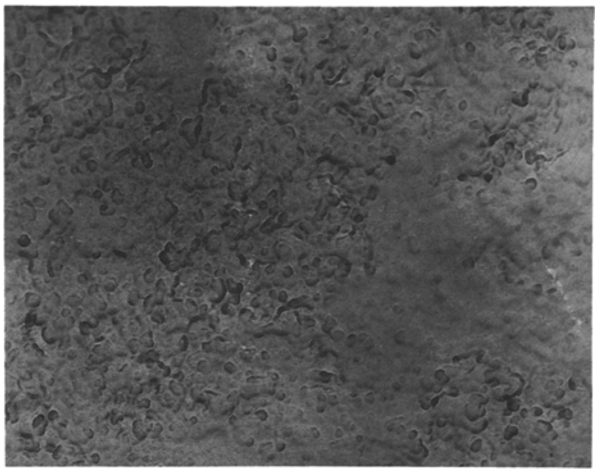

Figure 3 Photomicrograph of G4 heat treated at 600 °C for 1 h. Fine bulk crystallization of β-eucryptite ss and $\beta_{II'}$-Li_2ZnSiO_4 (crossed polars, × 60).

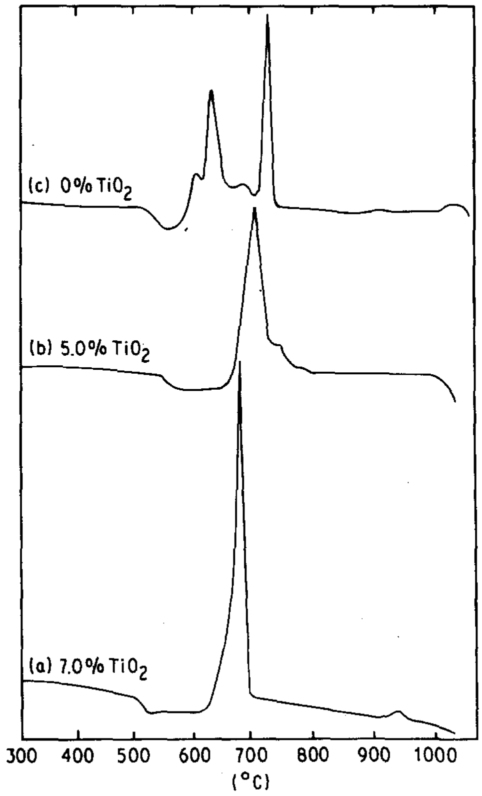

Figure 4 DTA curves of glasses with composition of 60% spodumene + 40% Li_2ZnSiO_4 nucleated with titania.

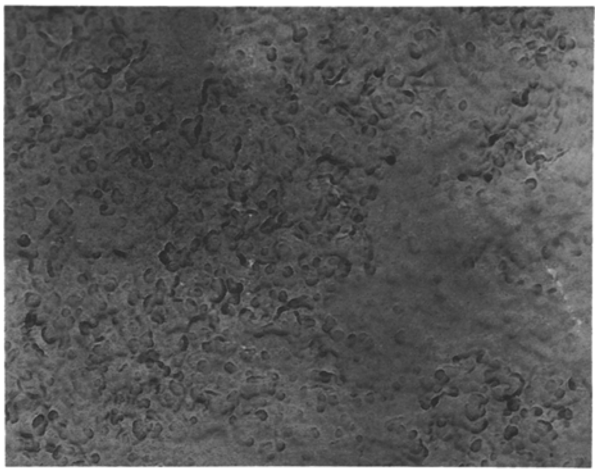

Figure 5 Replica electron micrograph of G4 + 7% TiO_2 after 5 h treatment at 540 °C. Liquid–liquid phase separation showing globular and oval-shaped droplets (× 25 000).

$\beta_{II'}$-Li_2ZnSiO_4 and facilitates the transformation of β-eucryptite ss to β-spodumene.

3.3. Crystallization of zirconia nucleated glasses

It can be easily seen from Fig. 8 and Table II that the endothermic and major exothermic peaks were progressively shifted to higher temperatures as the amount of ZrO_2 was increased.

Most of the 3% ZrO_2-containing glasses treated isothermally at temperatures up to 900 °C, through the one-step schedule, yielded incompletely crystalline materials. Only above 700 °C, and especially after pretreatment at the endothermic peak temperature even for only 1 h, intense bulk fine-grained crystallization took place readily throughout the whole sample. This may indicate that 3% ZrO_2 has a good nucleation effect on the crystallization process under such double-stage heat treatments. This catalytic effect on nucleation process, was exhibited in inducing homogeneous fine-grained microstructures. This effect was also proportional to ZrO_2 concentration in the glass (Figs 9 and 10).

The effect of different ZrO_2 concentrations, namely 0.5, 1.5 and 3.0%, on the type of crystalline phases developed in G4 composition is presented in Table III. ZrO_2 showed a significant catalytic effect on the $\beta_{II'} \rightarrow \gamma_0$-$Li_2ZnSiO_4$ transformation even at low-temperature treatments. ZrO_2 also favoured the crystallization of β-eucryptite ss and had a retarding effect on its transformation to β-spodumene.

4. Discussion

The effect of the Li_2ZnSiO_4 component, in lowering the temperature of the onset of crystallization and in inducing volume crystallization, could be ascribed to the well-known effect of Li_2O and ZnO in reducing the viscosity of the melts and their corresponding glasses [1, 11–13], a condition which weakens the

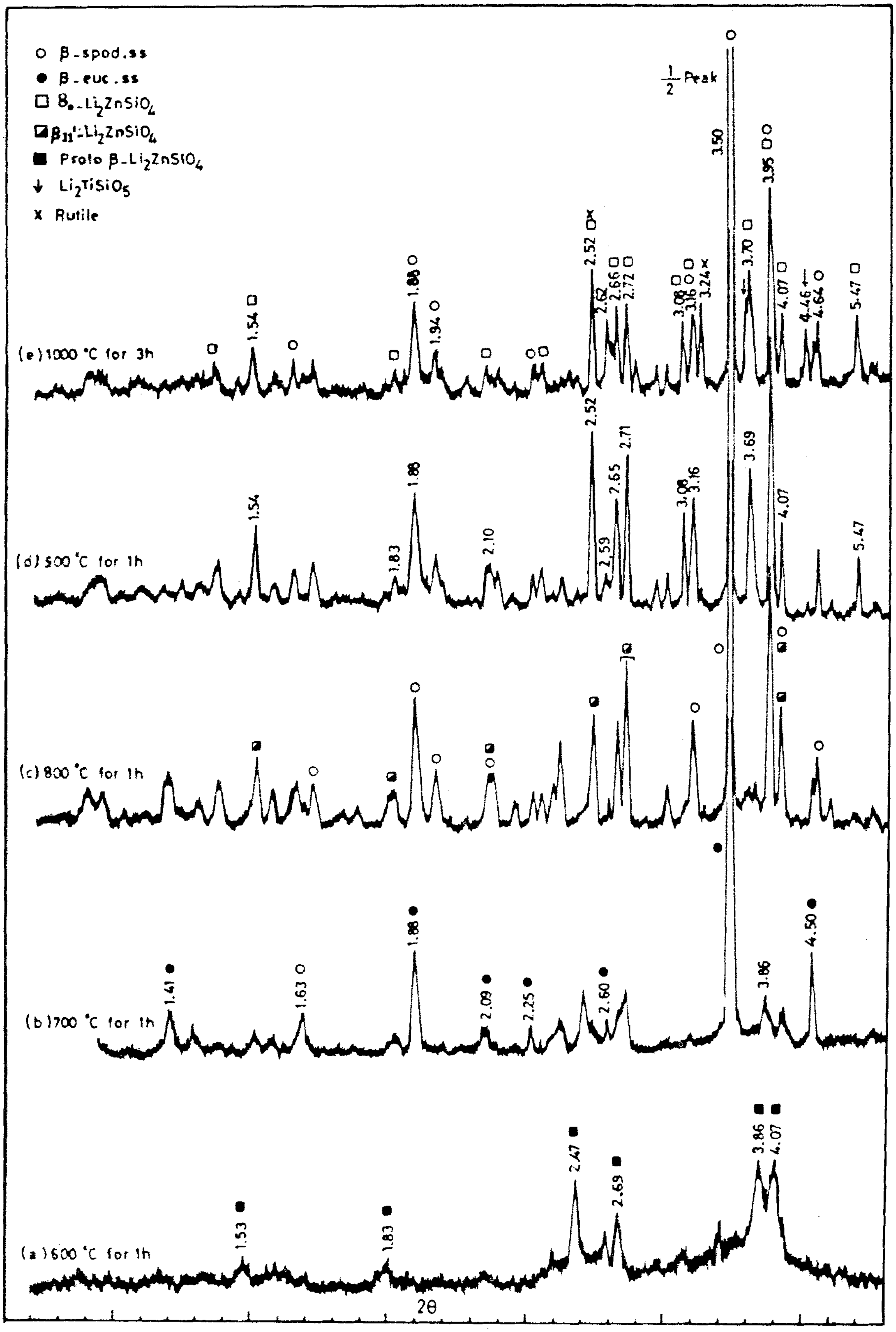

Figure 6 X-ray diffraction patterns of crystallized glasses with composition 60% spodumene + 40% Li_2ZnSiO_4 nucleated by 7% TiO_2.

structural bonds and facilitates the mobility and diffusibility of ions and structural elements in the glass, thus enhancing the crystallization process.

The ease of crystallization of such glasses, especially those rich in Li_2O and ZnO (G5), with the formation of fine-grained microstructures can be attributed to the incompatibility of the aforementioned modifying oxides with the glass-forming oxides SiO_2 and Al_2O_3 [11, 14]. These modifying oxides, having high electrostatic fields, in their attempt to screen themselves

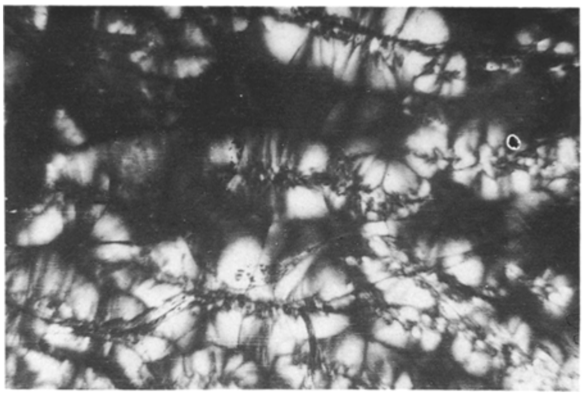

Figure 7 Replica electron micrograph of G4 + 7% TiO_2 heat treated at 700 °C for 1 h. Very dense population of quadrant and short prismatic crystallites forming a homogeneous ultra-fine microstructure. The sample is transparent in the visible spectrum (× 25 000).

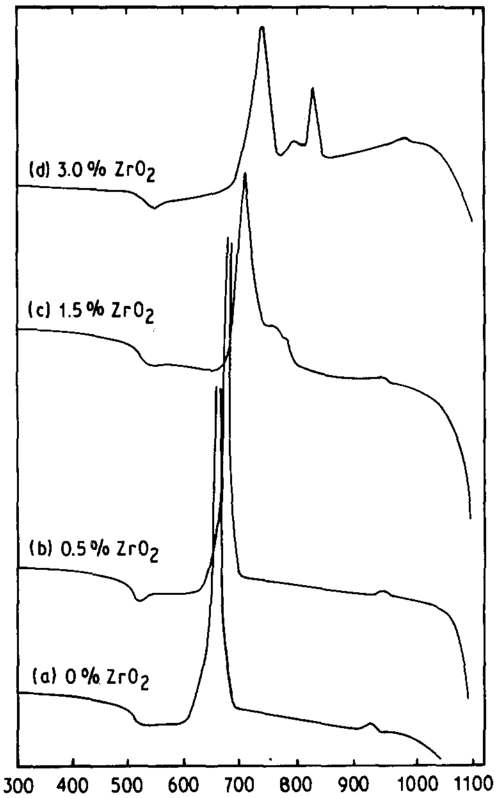

Figure 8 DTA curves of glasses with composition 60% spodumene + 40% Li_2ZnSiO_4 nucleated by zirconia.

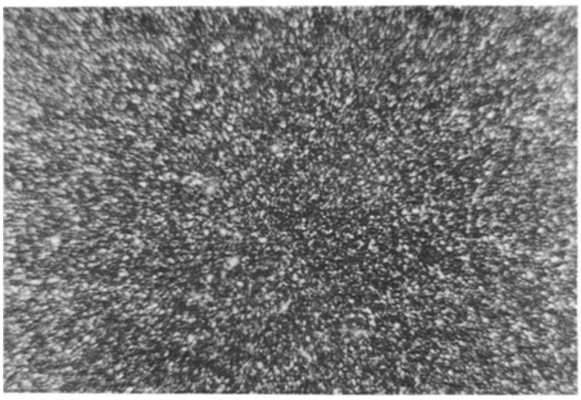

Figure 9 Photomicrograph of G4 + 1.5% ZrO_2 heat treated at 540 °C for 1 h and 780 °C for 1 h. β-eucryptite ss and an LiZn orthosilicate phase showing a uniform fine-grained sugary microstructure (crossed polars, × 60).

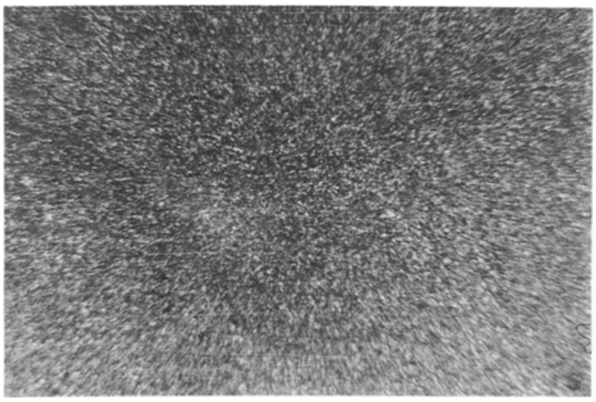

Figure 10 Photomicrograph of G4 + 3% ZrO_2 heat treated at 550 °C for 1 h and 790 °C for 1 h. Similar to the above but the crystals are ultra-fine. (crossed polars, × 115).

preferentially with non-bridging polarizable oxygen ions, tend to initiate liquid–liquid immiscibility in the glass which acts as nuclei for subsequent crystallization. It is generally agreed upon that one, or both, of the separated phases will be less stable toward devitrification than the original mother glass.

The type of resulting crystalline phases and microstructures was found to depend, to a great extent, upon the crystallization catalysts present in the glass. At the initial stages of crystallization, proto-β-Li_2ZnSiO_4 was formed over a relatively wider temperature range than in titania-free glasses. As a result of this trigger effect of TiO_2 on the formation of such proto-β-phase, transparent glass-ceramic materials could be easily obtained. The transparency is due to the ultra-fine grain size and the close similarity between the refractive indices of the proto-β crystallites and the surrounding residual glass as well as the low birefringence of the initially formed lithium aluminosilicate ss crystalline phase.

In consistence with the literature data [15, 16] TiO_2 favours the formation of β-spodumene and has a catalytic effect on the transformation of β-eucryptite ss into β-spodumene; and this effect increases with the increasing titania content. This may be attributed to the weakening effect of titanium on the network structure of glass [14, 17] which results in lower viscosity values and increased mobility of the glass structural elements. The relatively narrower temperature range of crystallization of β-eucryptite ss in titania-nucleated glasses is, therefore, due to the downwards displacement of its transformation temperature.

Different concepts and mechanisms were proposed to explain the role of TiO_2 in promoting fine-grained crystallization in different types of glasses [1]. It is generally agreed that TiO_2 leads to liquid unmixing (liquid–liquid phase separation) preceding internal or bulk crystallization [1, 16, 18]. The replica electron micrographs (Fig. 5) strongly and clearly support liquid–liquid phase separation during the heat treatment of the investigated titania-containing glasses. This may be followed by the separation of tiny crystallites of a zinc titanate spinellide phase which acts as a heterogeneous nucleation sites for the subsequent crystallization of the major phases; i.e. proto-β-Li_2ZnSiO_4 and β-eucryptite ss.

The promotion of volume crystallization in zirconia-containing glasses after double-stage heat treatments may be attributed to the enhancement of formation of Zr-bearing nucleation centres. Moriya *et al.* [19, 20] showed that the phases which first appeared in the Li_2O–Al_2O_3–SiO_2 system nucleated by ZrO_2 and TiO_2, were presumed to be cubic ZrO_2 or $ZrTiO_4$ crystals. The cubic ZrO_2 particles precipitate and increase in size with increasing heat-treatment temperature. When the diameter of these particles reaches 7 nm, crystals of β-quartz ss (20 nm diameter) were found to form suddenly over them.

The progressive formation of the γ_0-Li_2ZnSiO_4 with the increasing percentage of ZrO_2 in the glass may be due to the formation of a Zr-bearing nucleant phase similar in structure to the γ_0-phase which epitaxially nucleates and favours its formation. The effect of ZrO_2 on retarding the β-eucryptite ss → B-spodumene transformation is consistent with most literature data [3, 5, 16]. This effect may be related to the initially formed Zr-bearing nucleant phase as well as to the increase in the viscosity of the glass which consequently leads to less mobility of the structural elements in the glass to such an extent that the transformation between such complex aluminosilicate structures is delayed.

References

1. P. W. McMILLAN, "Glass-Ceramics", 2nd Edn (Academic Press, London, 1979).
2. S. D. STOOKEY, *Glastechen. Ber.* **32 K** (1959) 1.
3. D. R. STEWART, *Amer. Ceram. Soc. Special Pub.* **5** (1972) 41.
4. G. H. BEALL, B. R. KARSTETTER and H. L. RITTLER, *J. Amer. Ceram. Soc.* **50** (1967) 181.
5. A. W. A. EL-SHENNAWI, PhD thesis, Cairo University (1978).
6. A. R. WEST and F. P. GLASSER, *J. Mater Sci.* **5** (1970) 676.
7. *Idem., ibid.* **7** (1972) 895.
8. A. M. SHEHATA, PhD thesis, El-Menufya University, Egypt (1988).
9. A. A. OMAR, A. F. ABBAS and A. M. SHEHATA, *Rev. Int. Hautes Tempér. Réfract., Fr.* **24** (1987) 189.
10. A. W. A. EL-SHENNAWI, *J. Engng Sci.* **1** (1985) 1.
11. S. URENS, *Norwegian J. Chem. Mining. Met.* **21** (1961) 232.
12. P. S. ROGERS and J. WILLIAMSON, in "Proceedings of the 9th International Congress on Glass", France, edited by Institut du Verre, Paris, Section AL, 3 (1971) p. 141.
13. A. A. OMAR, *Egypt. J. Chem.* **15** (1972) 103.
14. M. TASHIRO, in "Proceedings of the 8th International Congress on Glass", London, edited by Society of Glass Technology, UK (1968) p. 113.
15. W. SACK and SCHEIDLER, *Glastech. Ber.* **39** (1966) 126.
16. A. W. A. EL-SHENNAWI, A. A. OMAR and A. A. MORSY, *Thermochim. Acta* **58** (1982) 125.
17. T. I. BARRY, D. CLINTON, L. A. LAY, R. A. MERCER and R. P. MILLER, *J. Mater Sci.* **4** (1969) 596.
18. S. M. OHLBERG, H. R. GOLOB and D. W. STICHLER, in "Symposium on the Nucleation and Crystallization of Glass Melts", edited by M. K. Reser, G. Smith and H. Insley (American Ceramic Society, Columbus, Ohio, 1962) p. 39.
19. Y. MORIYA, D. WARRINGTON and R. DOUGLAS, *Phys. Chem. Glasses* **8** (1967) 19.
20. Y. MORIYA, in "6th Symposium on Basic Ceramics", Osaka, Japan (1968).

Received 25 August 1989
and accepted 29 October 1990